

Introduction: Crater age-dating is the primary method of modeling surface ages across the solar system, and all are tied to the Moon from *Apollo* and *Luna* sample returns. Radiometric ages were determined for all landing sites with returns, and the most recent comprehensive work is by Stöffler & Ryder [1]. Craters on each sampled unit were counted and then related to the radiometric ages; this cratering chronology is often expressed as the sum of all craters $D \geq 1$ km on a given unit, $N(1)$, and that density corresponds with a certain age. Determining the $N(1)$ value for each unit requires detailed mapping of the locations on which samples were collected. This process has had a lengthy history, but almost all work was completed by 1980 [2-9], after which summaries were produced [10-12] and only a few have done any further work [13-15]. No one has published a comprehensive, uniform study of all calibration points, and no one has examined these sites with modern imagery and a current understanding of secondary craters, save the most recent <1 Ga points [15]. The purpose of this work is to reexamine the *Apollo* and *Luna* calibration sites and to derive a revised chronology, fitting the new $N(1)$ values to the determined radiometric ages.

Mapping and Crater Identification: LROC WAC (*Lunar Reconnaissance Orbiter* Camera Wide-Angle Camera) mosaics were created at near-native resolution (~ 60 mpp) of all the landing sites. For the three small crater calibration points (Cone, North Ray, and South Ray craters), LROC NAC (Narrow-Angle Camera) images were used (~ 0.5 mpp). The surfaces surrounding each site were conservatively mapped to only include the unit that was sampled, and craters $D \approx 0.5 - 10$ km were manually measured and cataloged. Each landing site was analyzed, and several comparison and consistency tests were conducted; the example of *Apollo 15* follows.

Example – *Apollo 15*: The *Apollo 15* landing site of the lunar module *Falcon* was close to Hadley Rille, on the eastern edge of the vast Mare Imbrium. This is one of the youngest of the lunar maria (estimated lava flooding at ~ 3.30 Ga and formation of the basin ~ 3.92 Ga [1]). The relatively small mare unit east of Hadley Rille was mapped along with a larger region of Mare Imbrium west of the rille (Fig. 1A).

The young, prominent Autolycus Crater is roughly 150 km north of the site, and some of the secondary craters from Autolycus were present within the mapped unit. Secondary craters are craters formed from cohesive ejecta blocks launched from the formation of a primary crater and are necessary to exclude from crater counts for age-dating purposes [18]. Of the 3353 km² mapped, 301 km² were excluded due to secondary craters.

Crater counts within the mapped area show $N(1) \approx$

5500 \pm 1300 (Fig. 1B). Given the uncertainties, the data overlap with previous results [6, 14] as well as historic raw data [6], although Neukum *et al.* [6] determined an $N(1)$ value substantially smaller than this study's, 3200 \pm 1100 likely because the $N(1)$ point was not measured directly in their work and so was based on an extrapolation. Recent crater counts by C. Fassett [pers. comm.] also overlap well, $N(1) = 5900 \pm 1600$. *Apollo 15* was a case where some of the original mapping images from the 1970s were available [6]. An independent analysis was performed with the archived *Apollo* metric camera images and the binned crater counts were found again to overlap well (Fig. 1B).

Other Sites: Overall, $N(1)$ of all sampling units in this work generally agree with previous results or are larger, indicating previous work under-counted or -estimated craters. The working hypothesis is this is due to most previous works extrapolating $N(1)$ rather than directly measuring it.

Results – Chronology Function: Determining both a fit function and parameters of that function to relate crater density with radiometric ages has had a long history that started with the first samples returned by *Apollo*. When all lunar sampling missions were completed with *Luna 24* and samples were dated, it was found there is a distinct lack of samples dating to >3.92 Ga and $\sim 1 - 3$ Ga, and so any fit is an extrapolation between $\sim 1 - 3$ Ga and is mostly unconstrained for >3.92 Ga [1]. Over time, consensus has evolved that a function with an exponential decline for ages ≥ 3.5 Ga and a linear rate thereafter is a reasonable fit to the data [e.g., 17, and references therein], though there remains the possibility of stochastic, unresolved spikes in the inner solar system cratering.

The work by Neukum *et al.* [17] is what is used by most people today, and their chronology relating $N(1)$ and time T is $N(1) = \alpha(\exp(-\beta T) - 1) + \gamma T$ where, for the Moon, $\alpha = 5.44 \cdot 10^{-14}$, $\beta = 6.93$, $\gamma = 8.38 \cdot 10^{-4}$. In scaling to Mars, α and γ are scaled down by ≈ 2.029 due to impact dynamics (gravity and impactor velocity). Scaling to other inner solar system bodies is done similarly, for it is assumed that the change in cratering rate has been relatively uniform between them. Since this function is defined for $N(1)$ and only $N(1)$, it is assumed that the impactor population has retained a constant size distribution. This assumption may not be accurate, but at the present time there is no consensus in this area and so it is assumed for this work to have remained constant with time. Hartmann *et al.* [13] proposed that, based on lunar impact melts from meteorites, *Apollo*-returned glass spherules, and Martian landslides, the classic time-scaling function be adjusted to include a quadratic term that reflects a decrease in the cratering rate over the past few billion years: $N(1) = \alpha(\exp(-\beta T) - 1) + \gamma T^2 + \delta T$.

This quadratic form was found to be a much better fit than the original linear form, and so it was fit with these new data (Fig. 2). After consideration of potentially questionable data points, the final fit parameters are: $\alpha = 2.607 \cdot 10^{-35}$, $\beta = 19.36$, $\gamma = 1.457 \cdot 10^{-4}$, $\delta = 1.038 \cdot 10^{-3}$. The reduced $\chi^2 = 1.70$. If one were to apply a dynamic correction for lunar apex/anapex cratering asymmetry [19], $\alpha = 2.335 \cdot 10^{-35}$, $\beta = 19.38$, $\gamma = 1.710 \cdot 10^{-4}$, $\delta = 1.010 \cdot 10^{-3}$, and reduced $\chi^2 = 1.56$.

Results – Implications: The qualitative consequences of these new fit parameters, in comparison with the established Neukum *et al.* [17] fit, are primarily three-fold: First, the smaller α parameter indicates the formerly linear term, now quadratic, dominates over more of geologic time; instead of the exponential dominating for $T > 3.3$ Ga, its effect is $T > 3.6$ Ga. Second, the larger β term increases the exponential significantly such that there is a very rapid increase in cratering as time into the past increases for as long as the function is valid, $T \leq 3.92$ Ga. Third, there are two points of intersection in the fits – 3.55 and 3.94 Ga – where surfaces have the same age at both, are older between, and surfaces are younger outside that range.

Figure 2C illustrates how ages change from [17] to the new chronology. For example, a surface dated to 3 Ga would move forward in time by nearly 1.1 Gyr, providing a new model crater age of 1.9 Ga. A surface dated to 3.6 Ga would have a revised model age 3.7 Ga. This acts to stretch many geologic processes on Mars closer to the present day while compressing earlier history – such as the extent of the lunar LHB – in time.

References: [1] Stöffler & Ryder (2001). [2] Shoemaker *et al.* (1970) in *Apollo 12 Prelim. Sci. Report*. [3] Soderblom & Boyce (1972) in *Apollo 16 Prelim. Sci. Report*. [4] Greeley & Gault (1970) doi: 10.1007/BF00561875. [5] Shoemaker *et al.* (1970) doi: 10.1126/science.167.3918.452. [6] Neukum *et al.* (1975) doi: 10.1007/BF00577878. [7] Neukum & Horn (1976) doi: 10.1007/BF00562238. [8] König (1977) thesis. [9] Moore *et al.* (1980) doi: 10.1009/BF00899820. [10] Neukum (1983) thesis. [11] Wilhelms (1987) "The Geologic History of the Moon." [12] Neukum & Ivanov (1994) ISBN 978-0816515059. [13] Hartmann *et al.* (2007) doi: 10.1016/j.icarus.2006.09.009. [14] Marchi *et al.* (2009) doi: 10.1088/0004-6256/137/6/4936. [15] Hiesinger *et al.* (2012) doi: 10.1029/2011JE003935. [16] Hartmann (2005) doi: 10.1016/j.icarus.2004.11.023. [17] Neukum *et al.* (2001). [18] McEwen & Bierhaus (2006) doi:10.1146/annurev.earth.34.031405.125018. [19] Le Fèvre & Wieczorek (2011) doi: 10.1016/j.icarus.2011.03.010. [20] placeholder

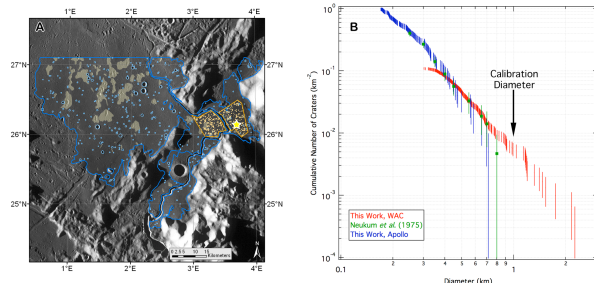


Figure 1: Example of the work done for every *Apollo* and *Luna 16* and *24* landing site, shown here for *Apollo 15*. Panel A shows the mapping from this work, outlined in blue, and regions of secondary craters that were removed from the mapping in translucent yellow. Orange outlines show regions mapped and craters measured in the same manner as some of the original work in this area [6]. Yellow star is the landing site. Panel B shows the cumulative size-frequency distributions (CSFD) with WAC and *Apollo* images from this and previous work [6]. For readability, the individual points on the CSFD from this work are represented only as a line indicating the uncertainty range. This is also a case where the $N(1)$ point was directly measured in this study, but it was clearly not covered with the older mapping.

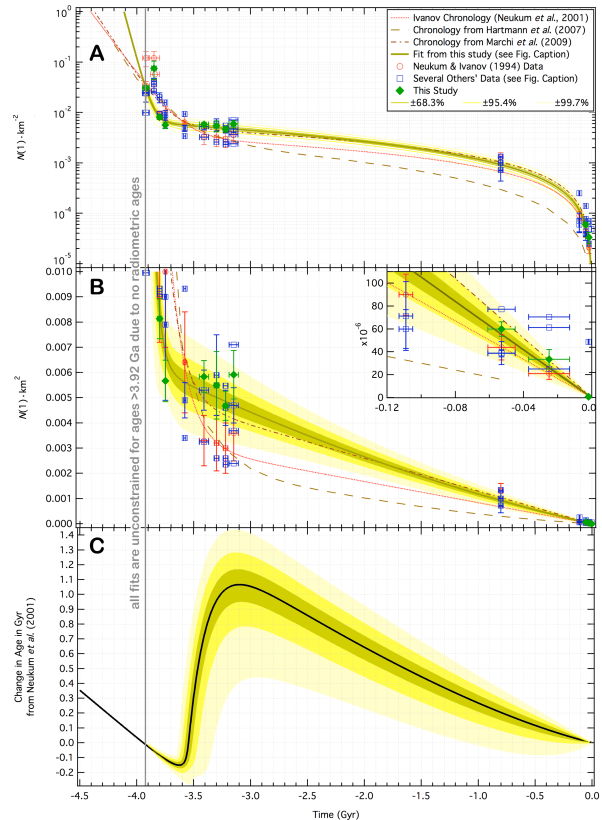


Figure 2: The canonical chronology [17] compared with revisions [13-14] and this work are in panels A and B. Panel A shows the function on semi-log axes, while Panel B focuses on the near-linear recent cratering rate on a linear plot with the last 120 Myr inset. The data points originally used by [10] and several comparison works [3-5, 8, 9-11, 14-15]. Panel C shows the difference between the new chronology and Neukum *et al.* [17] as a function of age in the old chronology. 1σ , 2σ , and 3σ confidence bands to the fit from this work are overlaid, and none of the fits are constrained for ages > 3.92 Ga.